

# RobustState: Boosting Fidelity of Quantum State Preparation via Noise-Aware Variational Training

Hanrui Wang<sup>\*1</sup>, Yilian Liu<sup>\*1</sup>, Pengyu Liu<sup>\*2</sup>, Jiaqi Gu<sup>3</sup>, Zirui Li<sup>1</sup>, Zhiding Liang<sup>4</sup>, Jinglei Cheng<sup>5</sup>,  
Yongshan Ding<sup>6</sup>, Xuehai Qian<sup>5</sup>, Yiyu Shi<sup>4</sup>, David Z. Pan<sup>3</sup>, Frederic T. Chong<sup>7</sup>, Song Han<sup>1</sup>

<sup>1</sup>MIT <sup>2</sup>CMU <sup>3</sup>University of Texas at Austin <sup>4</sup>University of Notre Dame

<sup>5</sup>Purdue University <sup>6</sup>Yale University <sup>7</sup>University of Chicago

**Abstract**—Quantum state preparation, a crucial subroutine in quantum computing, involves generating a target quantum state from initialized qubits. Arbitrary state preparation algorithms can be broadly categorized into arithmetic decomposition (AD) and variational quantum state preparation (VQSP). AD employs a predefined procedure to decompose the target state into a series of gates, whereas VQSP iteratively tunes ansatz parameters to approximate target state. VQSP is particularly apt for Noisy-Intermediate Scale Quantum (NISQ) machines due to its shorter circuits. However, achieving noise-robust parameter optimization still remains challenging.

There exist two types of noise-aware optimizers: gradient-free and gradient-based. Gradient-free optimizers, such as Bayesian optimization (BO), update parameters without gradient information, treating the problem as a black box. Gradient-based optimizers, on the other hand, utilize gradients derived from the parameter shift (PS) rule. Both approaches suffer from *low training efficiency*: gradient-free optimizers lack accurate gradient guidance, and PS demands a costly  $\mathcal{O}(N)$  executions for  $N$  parameters. While existing noise-unaware optimizers can exploit back-propagation on a classical simulator for efficient gradient computation in a *single* backward pass, they exhibit *low robustness* on real machines.

We present RobustState, a novel VQSP training methodology that combines high robustness with high training efficiency. The core idea involves utilizing measurement outcomes from real machines to perform back-propagation through classical simulators, thus incorporating real quantum noise into gradient calculations. RobustState serves as a versatile, plug-and-play technique applicable for training parameters from scratch or fine-tuning existing parameters to enhance fidelity on target machines. It is adaptable to various ansatzes at both gate and pulse levels and can even benefit other variational algorithms, such as variational unitary synthesis.

Comprehensive evaluation of RobustState on state preparation tasks for 4 distinct quantum algorithms using 10 real quantum machines demonstrates a coherent error reduction of up to  $7.1 \times$  and state fidelity improvement of up to 96% and 81% for 4-Q and 5-Q states, respectively. On average, RobustState improves fidelity by 50% and 72% for 4-Q and 5-Q states compared to baseline approaches.

## I. INTRODUCTION

Quantum Computing (QC) is emerging as a promising computing paradigm, garnering significant research interest for addressing previously unsolvable problems with enhanced efficiency. Various industries and disciplines stand to benefit from QC, including cryptography [81], database search [28], combinatorial optimization [19], molecular dynamics [71], and

<sup>\*</sup>Equal Contributions.

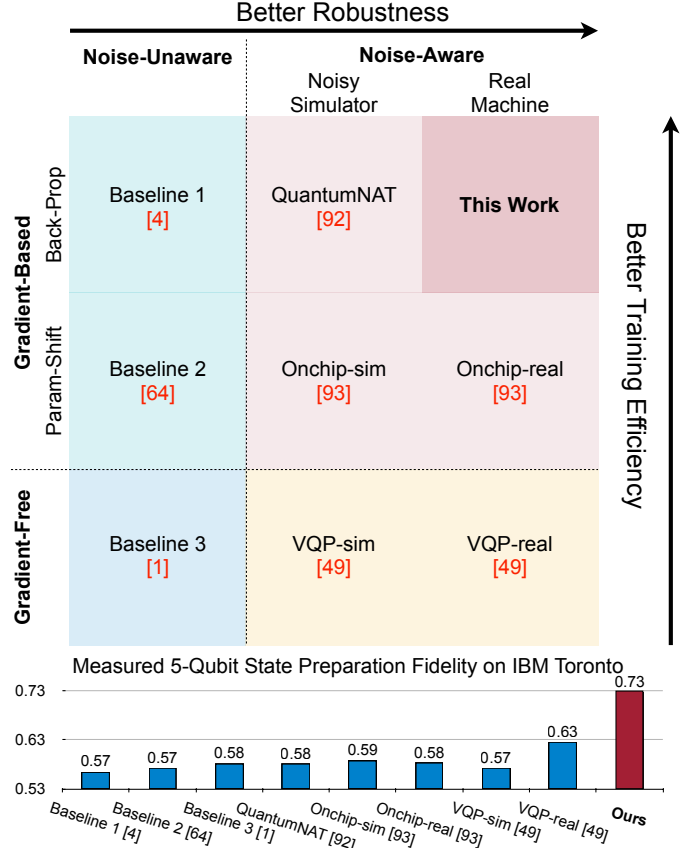


Fig. 1. Proposed RobustState performs back-propagation training using results from real quantum machines, achieving high robustness and training efficiency. State preparation fidelity of each method is evaluated on real machines.

machine learning [5], [50], [54], [77], among others. Progress in physical implementation technologies has spurred rapid advancements in QC hardware over the past two decades, leading to the recent release of multiple QC systems with up to 433 qubits [33], [35], [39], [78].

Quantum state preparation, a crucial subroutine in QC, facilitates the preparation of the system's initial state. This process is essential for applications such as codewords in quantum error correction [32], amplitude encoding [69] in quantum machine learning, and initial condition loading for solving Partial Differential Equations (PDEs) using quantum machines [25], [56].

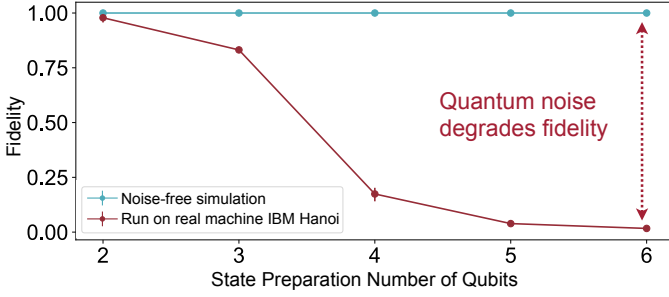


Fig. 2. Prepared state fidelity on a noise-free simulator and real machine IBM Hanoi. (i) Noise-free fidelity is very close to 100%. (ii) Noise significantly reduces fidelity, especially for large qubit numbers.

State preparation can be achieved through two primary approaches: arithmetic decomposition (AD) and variational quantum state preparation (VQSP). AD methods, such as Shannon decomposition [58] and Mottonen decomposition [66], focus on generating circuits to prepare the target state. Shannon decomposition, inspired by Shannon’s expansion theorem in classical reversible computing, constructs a quantum circuit by first synthesizing a series of classical reversible gates and subsequently translating them into quantum gates [58]. Mottonen decomposition, in contrast, decomposes the target state into single-qubit rotations and multi-qubit controlled rotations [66]. This process iteratively constructs the target state hierarchically, beginning with the least significant qubit and progressing with each layer of controlled rotations acting on an increasing number of qubits. The second approach, variational quantum state preparation (VQSP) [2], [12], employs a different strategy by iteratively updating parameters in a variational circuit ansatz. This iterative process aims to minimize the distance between the implemented final state and the target state.

On NISQ machines, AD methods can be significantly affected by quantum noise. Utilizing IBM Qiskit [1] compiler for Shannon decomposition, we generate circuits that transform the all-zero state into three distinct quantum states and compare the average fidelity on noise-free simulators and real quantum machines (Fig. 2). Although the compiler can achieve 100% fidelity in noise-free simulations, real quantum machines experience considerable fidelity degradation. This fidelity gap intensifies with an increasing number of qubits, e.g., while 2-qubit (2-Q) states achieve 98% fidelity on real machines, 6-qubit (6-Q) states have a mere 1% fidelity. Conversely, VQSP is better suited for NISQ devices due to its flexibility in mitigating coherent errors by adjusting circuit parameters and its reduced 2-qubit gate count and depth, as observed in our experiments.

Nevertheless, Optimizing VQSP parameters for *noise robustness* remains a formidable challenge. Fig. 1 presents a taxonomy of existing optimization strategies for parameter training and their performance on a 5-qubit (5-Q) quantum state on the IBM Toronto machine. Although noise-free fidelities exceed 99%, fidelity on real machines significantly declines. The performance of noise-unaware simulation methods in the first

column, such as training on a noise-free simulator, deteriorates due to real machine noise. In the second column, training with noisy simulators like QuantumNAT [92], onchip-sim [93], and VQP-sim [49], still results in low state fidelity on real devices due to discrepancies between the simulator and the actual device. Despite that, training on classical differentiable noise-free or noisy simulators is *faster than black-box* optimizers for achieving the same fidelity level, as accurate gradients for all parameters can be computed in a *single* backward pass. The rightmost column outlines optimization methods using real machines. Gradient-free optimizers, such as Bayesian optimization, update parameters with reward feedback from real devices, while gradient-based optimizers update parameters with gradients computed from the parameter shift (PS) rule executed on real machines. Regrettably, both methods suffer from low training efficiency. Gradient-free optimizers treat the problem as a black box, lacking accurate gradient guidance, and PS, despite providing gradient guidance, incurs high costs, necessitating  $\mathcal{O}(\#params)$  executions for a single parameter update round.

The natural goal of achieving both high robustness and training efficiency calls for *noise-aware back-propagation*. However, due to the No-Cloning Theorem [17], [98], back-propagation on real quantum machines is infeasible, as intermediate results (quantum states) cannot be stored for use in the backward pass.

To address this challenge, we introduce RobustState. The core idea hinges on the fact that while real quantum machines cannot provide intermediate results, they can supply *final results* through measurements. Thus, we can use final results from real quantum machines combined with intermediate results from classical simulators to complete the backward pass. In a single training step, the same set of parameters is executed on *both* real quantum machines and simulators. The loss function is computed between the tomography states from a real machine and the target state. Subsequently, noise-impacted gradients are back-propagated through the simulator using the previously simulated intermediate results, ensuring noise resilience in the trained parameters. Fig. 1 (bottom) highlights the superior accuracy of our method over alternatives. The two primary advantages of our approach are summarized in Table I.

RobustState balances increased classical computation in simulators against reduced executions on real devices and enhanced fidelity by obtaining gradients for all parameters with one tomography. While classical simulation scalability may be a concern, we argue the following points: (i) The scalability of our approach is *comparable* to that of state-of-the-art arithmetic decomposition methods [58], [66], yet it attains significantly higher fidelity. (ii) Preparing small to medium-sized states with high fidelity is a crucial task in quantum computing. For instance, the five-qubit code [26] and nine-qubit surface code [20] are essential starting procedures for all programs in fault-tolerant quantum computing [9], [13], [75], [87], [100]. (iii) Block-wise optimized quantum circuit compilers, such as [103], benefit significantly from generating unitaries for a few qubits with high fidelity, as this serves as a crucial subroutine for improving the final circuit fidelity. Thus

	Parameter-Shift Gradient-Free RobustState		
Scaling w.r.t. #Params	$\mathcal{O}(n)$	Unscalable	$\mathcal{O}(1)$
Gradient Guidance	✓	✗	✓

TABLE I  
COMPARISON BETWEEN DIFFERENT NOISE-AWARE OPTIMIZERS.

the potential scalability concerns of classical simulators are outweighed by the value and importance of preparing small to medium-sized states with high fidelity.

RobustState offers a plug-and-play approach capable of enhancing the fidelity of any existing ansatz, such as those from Xanadu [56] and QuantumNAS [91]. Unlike traditional PS rules, which necessitate specific quantum gate structures [64] for gradient computation, RobustState calculates gradients through a simulator, eliminating the need for particular ansatz structures and ensuring broad applicability to any classically simulatable ansatz. Consequently, our method can be employed to improve the performance of *both gate and pulse* ansatzes, as demonstrated in our experiments. Moreover, the noise-aware back-propagation technique can be extended to other variational algorithms, highlighting its wide-ranging applicability and effectiveness. Our experiments involving variational unitary synthesis and quantum state regression provide further evidence of its extensive utility. In summary, RobustState makes the following contributions:

- **Noise-aware gradient back-propagation approach:** This method enhances both the robustness and training efficiency of variational state preparation circuits.
- **Extensive applicability across various ansatzes and applicable to other variational algorithms:** RobustState is applicable at both gate and pulse levels and is compatible with existing ansatz design and search frameworks. The methodology can also be applied to other variational algorithms such as unitary synthesis and quantum state regression.
- **Comprehensive experiments on 10 real machines:** Our results demonstrate that RobustState improves 4-Q state fidelity by **50%** and 5-Q state fidelity by **72%** on average, reducing coherent errors by up to **7.1×** when compared to noise-unaware baselines.

## II. VARIATIONAL QUANTUM STATE PREPARATION

In this section, we briefly introduce several concepts used in variational quantum state preparation.

**Quantum state preparation.** Grover and Rudolph initially introduced the quantum state preparation problem for efficiently generating integrable probability distribution functions [27]. Numerous state preparation techniques have been proposed since, targeting specific states like Gaussian wave functions [3], [40], [74], continuous functions [31], [73], and arbitrary functions [61], [72], [84], [106]. State preparation techniques can be categorized into Arithmetic Decomposition (AD) and Variational Quantum State Preparation (VQSP). AD utilizes rule-based algorithms to generate a circuit mapping the  $|0\rangle$  state to the target state  $|\psi\rangle$  in one step, while VQSP iteratively refines a circuit to minimize the difference between the

produced and target states. VQSP begins with designing a parameterized circuit architecture (called ansatz). The circuit realizes a parameterized unitary  $U(x, \theta)$ , preparing a state:  $|\psi(x, \theta)\rangle = U(x, \theta)|0\dots 0\rangle$ , where  $x$  is the input data for computation, and  $\theta$  is a set of free variables for adaptive optimizations. A set of circuit parameters are then trained using a hybrid quantum-classical optimization procedure, iteratively updating parameters in  $U(x, \theta)$  to minimize loss.

**Hardware-efficient ansatz.** Although AD can prepare arbitrary quantum states precisely in theory, practical application is limited on real machines due to topological constraints and significant hardware noise. Exact preparation schemes require all-to-all connectivity between qubits, so additional SWAP gates are needed for real-machine deployment. To address these issues, researchers proposed hardware-efficient ansatzes [23], [38] that use only native (or near-native) gates provided by a specific backend to produce compact, expressive circuits. More compact circuits are more robust against noise, so we base our framework on variational quantum circuits to tackle topological constraints and hardware noise.

**Quantum state fidelity.** Quantum state fidelity measures how closely two states match, defined as  $F(\rho, \sigma) = (\text{tr} \sqrt{\sqrt{\rho}\sigma\sqrt{\rho}})^2$ , where  $\sqrt{\rho} > 0$  and  $(\sqrt{\rho})^2 = \rho$ . If either  $\rho$  or  $\sigma$  is a pure state, fidelity simplifies to  $F(\rho, \sigma) = \text{tr}(\rho\sigma)$ . If  $F(\rho, \sigma) = 1$ ,  $\rho$  and  $\sigma$  are identical. We will use fidelity as a prepared state quality indicator throughout this paper.

**Incoherent and coherent noises.** On real quantum computers, errors arise from qubit-environment interactions and imprecise controls [8], [42], [59]. Qubit-environment interactions lead to quantum state information loss, termed *incoherent errors*, expressed mathematically as  $|\phi\rangle\langle\phi| \rightarrow (1-p)|\phi\rangle\langle\phi| + p\frac{I}{d}$ , where  $p$  represents incoherent error strength. Imprecise quantum gate controls cause coherent errors, where the state vector deviates from the ideal state vector:  $|\phi\rangle\langle\phi| \rightarrow |\phi'\rangle\langle\phi'|$ .

Coherent errors can be mitigated through software approaches. Characterization [59] and calibration [36] are two standard methods to estimate and reduce coherent errors. However, even with calibration, coherent errors cannot be entirely eliminated. In state preparation, we model errors as a combination of incoherent and coherent errors. Assuming we aim to prepare state  $\rho = |\phi\rangle\langle\phi|$  but obtain  $\rho' = (1-p)|\phi\rangle\langle\phi| + p\frac{I}{d}$ , where  $p$  signifies incoherent error strength, and  $|\phi\rangle \neq |\phi'\rangle$  indicates coherent error. We quantify coherent error using the infidelity between  $|\phi\rangle$  and  $|\phi'\rangle$ . With simple derivations, we can approximate coherent error as:

$$1 - \frac{\text{tr}(\rho\rho')}{\sqrt{\text{tr}(\rho^2)}} \quad (1)$$

## III. NOISE-AWARE ROBUSTSTATE METHODOLOGY

In this section, we first discuss the advantages of using variational state preparation over conventional arithmetic decomposition. Next, we introduce the RobustState approach for noise-aware back-propagation parameter training. Finally, we discuss the extensive applicability of RobustState on both gate and pulse ansatzes.

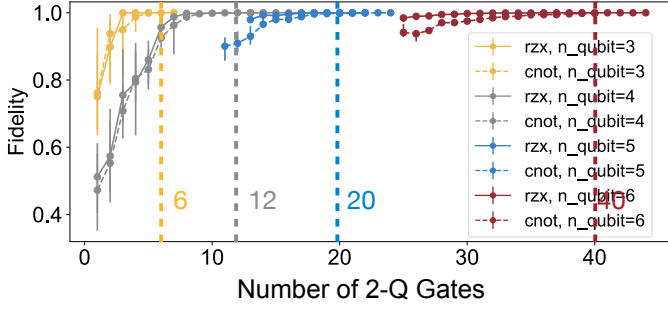


Fig. 3. Noise-free state fidelity for 3-Q, 4-Q, 5-Q, and 6-Q states versus the number of 2-Q gates. Each ansatz is tested with both CNOT and RZX as the 2-Q gate.

	3-Q	4-Q	5-Q
MEAN(fidelity)	0.9996	0.9988	0.9998
STD(fidelity)	0.0013	0.0015	0.0003

TABLE II

NOISE-FREE FIDELITY FOR ARBITRARY STATES AFTER THE CONVERGENCE OF HARDWARE-EFFICIENT VQSP ANSATZ.

#### A. Arithmetic Decomposition versus Variation State Preparation

We conduct experimental comparisons between arithmetic decomposition and variational approaches. For AD, we employ Qiskit’s `initialize` method and the Mottonen decomposition method [66]. For VQSP, we choose ansatzes with sufficient expressibility by examining the fidelity when using varying numbers of 2-Q gates. As the number of 2-Q gates increases, the ansatz’s expressibility becomes adequate for generating any quantum state. We use hardware-efficient ansatzes to ensure no extra SWAP gates are required. As demonstrated in Fig. 3, we ensure the ansatz converges to the target state by selecting 6 2-Q gates for 3-Q states, 12 for 4-Q states, and 20 for 5-Q states. Table II presents the mean and standard deviation for the fidelity of chosen ansatzes for 100 randomly generated states. The means all exceed 99% with standard deviations smaller than 0.002, indicating the ansatzes’ sufficient expressibility.

Then, we compare the 2-Q gate count of VQSP circuits, achieving nearly 100% fidelity with circuits generated by Qiskit’s `initialize` method and the Mottonen method in Fig. 4. The 2-Q gate counts for the two AD methods increase after compiling to specific hardware due to the insertion of SWAP gates, while our counts remain unchanged. It is evident from the figure that variational state preparation requires fewer 2-Q gates, with reductions exceeding  $6\times$  for 6-Q states. Thus, we conclude that variational approaches are preferable for generating small-size, high-fidelity circuits.

#### B. Noise-Aware Back-Propagation with RobustState

Although variational circuits are smaller, they necessitate iterative parameter training. As discussed in Sec. I, noise-aware back-propagation is the optimal candidate for achieving high robustness and training efficiency. However, real quantum machines cannot perform back-propagation due to quantum mechanics’ fundamental limits, specifically the No-Cloning

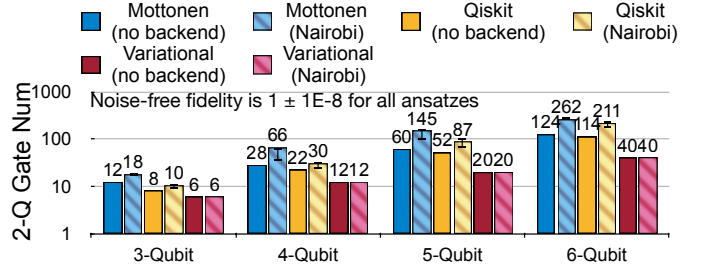


Fig. 4. The VQSP ansatz has much fewer 2-Q gates but achieves similar noise-free fidelity (100%) compared with the arithmetic decompositions (Mottonen and Qiskit).

#### Algorithm 1: RobustState Training with Noise-Aware Gradient Back-Propagation

**Input** : Training objective  $\mathcal{L}$ , quantum real machine execution function  $f(\cdot)$ , classical simulation function  $f'(\cdot)$ , initial parameters  $\theta^0 \in \mathbb{R}^n$ , initial learning rate  $\eta^0$ , and total steps  $T$ .

```

 $\eta \leftarrow \eta^0$ ;
for  $t = 0, 1, \dots, T-1$  do
    Execute circuit on real quantum machine
     $\rho = f(\theta^t)$ ;
    Simulate circuit on classical simulator
     $\rho' = f'(\theta^t)$ ;
    Objective evaluation with noisy output:  $\mathcal{L}(\rho)$ ;
    Classical backpropagation to obtain noisy gradients
     $\nabla_{\theta^t} \mathcal{L}(\rho) = \frac{\partial \mathcal{L}(\rho)}{\partial \rho} \frac{\partial \rho}{\partial \theta^t}$ ;
    Parameter update:
     $\theta^{t+1} \leftarrow \theta^t - \eta \nabla_{\theta^t} \mathcal{L}(\rho)$ ;
end
Output : Converged parameters  $\theta^{T-1}$ 

```

Theorem [17], [98], which prevents storing intermediate results necessary for back-propagation. Fortunately, the final results (density matrix) of quantum circuits can be obtained through measurements, providing abundant noise information. Inspired by [99], we employ a differentiable classical simulator to acquire intermediate results (quantum states) so that back-propagation can be performed using the noisy final output and simulated intermediate results. In Alg.1, we outline the RobustState training protocol, which combines quantum on-chip forward with classical simulated backward propagation for noise-aware gradient-based optimization. This process is graphically illustrated in Fig.5. In each iteration, we first execute the quantum circuits on the real quantum device and perform tomography to obtain the density matrix  $\rho$ , which incorporates the effects of real noises. Next, we simulate the quantum circuit on classical computers to obtain a noiseless density matrix  $\rho'$ . To adjust parameters based on a specific machine’s noise, we *replace* the noiseless density matrix  $\rho'$  with the noisy one  $\rho$  to evaluate the loss function  $\mathcal{L}(\rho)$ .

**Noisy gradient back-propagation.** During back-prop, we adopt straight-through estimator (STE) that directly passes the noisy gradient  $\frac{\partial \mathcal{L}(\rho)}{\partial \rho}$  to the theoretical noise-free path,



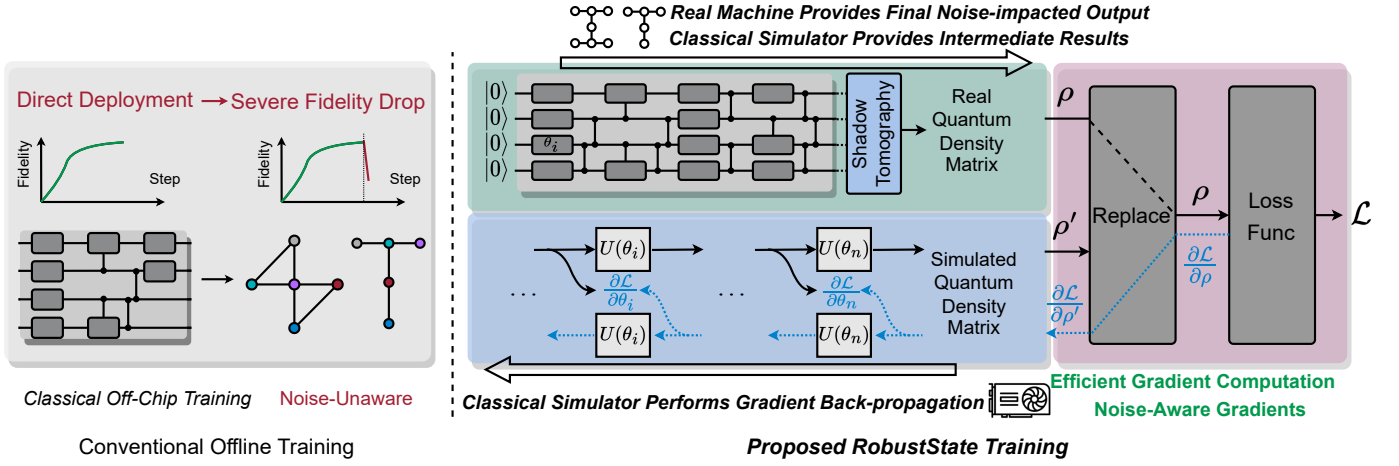


Fig. 5. RobustState with real noise-aware gradients improves parameter robustness.

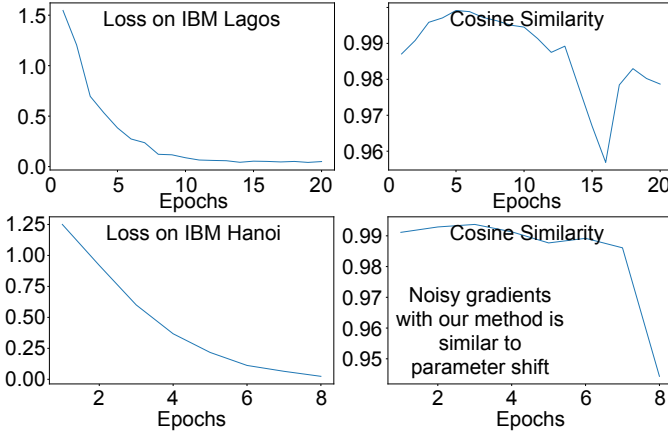


Fig. 6. Noise-aware gradients approximated with RobustState are close to the accurate ones computed with the parameter shift rule.

i.e.,  $\frac{\partial \mathcal{L}(\rho)}{\partial \rho} \rightarrow \frac{\partial \mathcal{L}(\rho)}{\partial \rho'}$ . Then, this estimated noisy gradient will be used to calculate derivatives for all parameters  $\frac{\partial \mathcal{L}(\rho)}{\partial \theta} = \frac{\partial \mathcal{L}(\rho)}{\partial \rho'} \frac{\partial \rho'}{\partial \theta}$ . The fundamental reason why this gradient replacement works is that the quantum noise information can be effectively coupled in the back-propagation procedure, i.e., the noisy upstream gradient  $\frac{\partial \mathcal{L}(\rho)}{\partial \rho}$ , to make the training process fully aware of real quantum noises. Note that this property requires the objective  $\mathcal{L}(\cdot)$  to be a nonlinear function of the noisy  $\rho$ . Otherwise,  $\frac{\partial \mathcal{L}(\rho)}{\partial \rho}$  will only contain noise-free terms. This methodology synergistically leverages the noise awareness of real quantum machines and the differentiability of classical simulators for parallel, highly efficient noise-aware training.

We will illustrate this hybrid training idea with a concrete example. In our experiments, we choose the loss function to be  $\mathcal{L} = \sqrt{\text{tr}((\rho - \hat{\rho})^2)}$ , then  $\nabla_{\theta} \mathcal{L} = \text{tr}\left(\frac{(\rho - \hat{\rho})}{\mathcal{L}} \frac{\partial \rho'}{\partial \theta}\right)$ . After the parameter update, the state becomes

$$\rho_{t+1} = \rho_t - \sum_{\theta} \frac{\eta}{\mathcal{L}_t} \text{tr}\left((\rho_t - \hat{\rho}) \frac{\partial \rho'}{\partial \theta_t}\right) \frac{\partial \rho}{\partial \theta_t} + O(\eta^2), \quad (2)$$

then the loss function becomes

$$\mathcal{L}_{t+1}^2 - \mathcal{L}_t^2 = -2 \sum_{\theta} \frac{\eta}{\mathcal{L}_t} \text{tr}\left((\rho_t - \hat{\rho}) \frac{\partial \rho'}{\partial \theta_t}\right) \text{tr}\left((\rho_t - \hat{\rho}) \frac{\partial \rho}{\partial \theta_t}\right) + O(\eta^2). \quad (3)$$

As long as  $\frac{\partial \rho}{\partial \theta_t} \approx \frac{\partial \rho'}{\partial \theta_t}$  and the learning rate  $\eta$  is small enough, the two  $\text{tr}(\cdot)$  operators will have the same sign with high probability and  $\mathcal{L}_{t+1} < \mathcal{L}_t$ .

We further compare hybrid training approximated gradients with the real gradients estimated by parameter shift to show experimental evidence of our method's effectiveness. We build a 3-Q ansatz with 2 RX gates on qubits 0 and 2 and an RY gate on qubit 1, followed by three RZX gates connecting qubits 0 and 1, 1 and 2, 2 and 0. So there are 6 trainable parameters in total. After each training step, we compare the cosine similarity of gradients between the two methods. Note that we adjust the loss function from comparing the state vector to comparing the expectation values of the Pauli-Z measurement. As in Fig. 6, the similarities are higher than 0.95. Therefore, our method can provide accurate noise-aware gradients while reducing the  $\mathcal{O}(\# \text{parameters})$  circuit executions in parameter shift to  $\mathcal{O}(1)$  complexity per round.

The RobustState is a plug-and-play approach that can be used. We note that our noise-aware gradients may not be necessary at the beginning of the training when parameters are far from convergence. Thus, in real experiments, we can combine this noise-aware training with pure classical training by first training the parameters to convergence in a simulator and then performing parameter fine-tuning using noise-aware training to reduce the cost of running on real machines. Furthermore, by replacing the loss function, our method can be used for other variational quantum algorithms to further boost the tasks' performance. We will illustrate this using unitary synthesis and quantum state regression below.

**Quantum tomography.** To get feedback from real machines, our method needs to know the prepared state  $\rho$  on real machines while optimizing parameters to suit the specific noise pattern. This can be done by quantum state tomography. Among

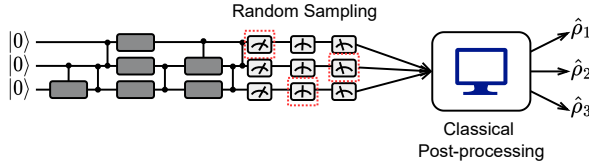


Fig. 7. Sketch of the classical shadow tomography. In classical shadow tomography, we measure on random bases. After classical post-processing, each measurement result generates a snapshot of  $\rho$ ,  $\hat{\rho}_i$ , which is an unbiased estimation of  $\rho$ , i.e.  $\mathbb{E}(\hat{\rho}_i) = \rho$ . With sufficient number of measurements, we can approximate  $\rho$  using  $\frac{1}{n} \sum_i \hat{\rho}_i$ .

many kinds of tomography methods, we choose to use the classical shadow tomography [34] to estimate the prepared state as shown in Fig. 7. Compared with traditional tomography methods like the one implemented in Qiskit [82], classical shadow tomography provides an unbiased estimation of the state  $\rho$  with any number of measurements. This feature allows us to sample some state bases and update the parameters without performing a full state tomography with  $3^n$  circuits. This sampling is an analog of SGD and can relieve the scalability issue, as discussed in the last paragraph of Sec. IV-C. We also adopt the readout error mitigation technique proposed in [57], which prevents ansatzes from minimizing the loss function by overfitting the readout error pattern.

### C. Extensive Applicability of RobustState

As discussed in the previous subsection, RobustState requires no assumption on the ansatz structure. It applies to all kinds of quantum operations with analytical formulations, while the parameter shift rule is only narrowly applicable to gates whose unitary has a structured eigenvalue [64]. So our method can be directly combined with existing ansatz design such as Xanadu [2] and QuantumNAS [91] to boost their fidelity. It can also be utilized on pulse-level ansatz to further compress the circuit depth.

Pulse-level control introduces more parameters compared to gates, which enables abundant opportunities for a more compact ansatz [23]. We can generate two more parameterized basis gates, the  $RX(\theta)$  and  $RZX(\theta)$  gates which are shown in Fig. 8, without any calibration cost using pulse level control. To implement  $RX(\theta)$  from existing calibration data, we retrieve the pulse shape of the pre-calibrated X gate and adjust the pulse amplitude by setting the area under the curve proportional to  $\theta$ . According to the basic principle of quantum dynamics, it is an approximation of  $RX(\theta)$ . Similarly, we retrieve the pulse shape of the pre-calibrated CR, and adjust the area under it to implement  $RZX(\theta)$  for any  $\theta$ .

Using a native pulse gate set has several benefits. An arbitrary single qubit rotation will be decomposed to up to 5 native gates for IBM's default implementation (RZ, SX, RZ, SX, RZ). However, with native pulse gates, we can reduce this number to 3 (RZ, RX, RZ) [24]. With regards to RZX gates, the entanglement operation between qubits can be precisely controlled. Thus, the circuit requires shorter runtime and has more parameters with better expressivity.

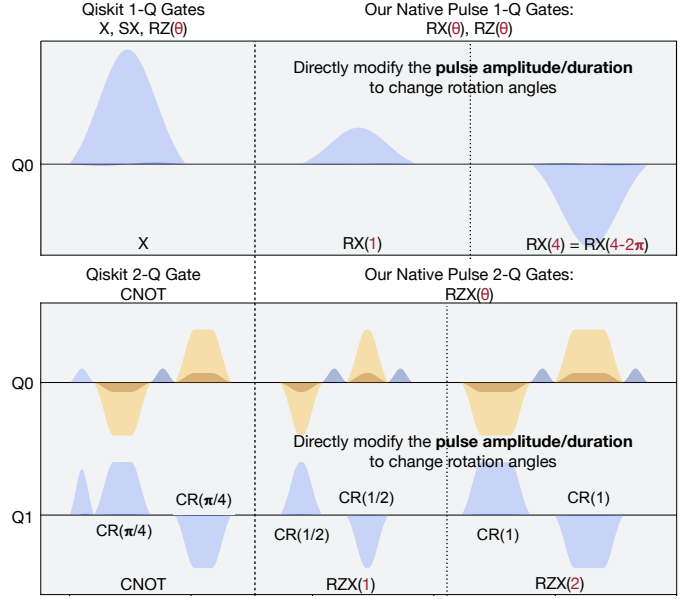


Fig. 8. Pulse schedules for X, RX (1) and RX (4) (top); CNOT, RZX (1) and RZX (2) (bottom). For IBM's quantum computers, calibration is only performed for X, SX, and CNOT, so we need to adjust the pulse shape to generate RX ( $\theta$ ) and RZX ( $\theta$ ) for arbitrary angles.

It should be noted that changing the amplitude of the pre-calibrated pulse only provides an approximation of rotation gates. Due to the imperfection of classical control and the influence of higher energy-level in superconducting quantum computers, the system is not entirely linear [21]. For example, the amplitude of SX might not be exactly half that of the X gate. Take IBMQ Jakarta as an example. The pulse amplitude of SX and half the amplitude of X has about 0.9% relative difference, which introduces a detectable amount of coherent error when simply adjusting the pulse proportionally without any fine-tuning. Thankfully, our noise-aware training method in III-B can automatically correct these coherent errors. With shorter pulse duration, the fidelity of the state can be improved.

## IV. EVALUATION

### A. Evaluation Methodology

As explored in earlier sections, the present study examines RobustState in relation to existing state preparation methodologies across three distinct dimensions. Firstly, the analysis demonstrates that RobustState, functioning as a variational framework, surpasses the performance of AD algorithms, as illustrated in Fig. 11. Subsequently, RobustState is compared to alternative variational approaches concerning training efficiency and noise-robustness, as depicted in Fig. 12 and Fig. 13. The findings reveal that, by exhibiting the highest degree of training efficiency and noise-robustness, RobustState outperforms all other variational techniques under investigation.

Four categories of representative target states with 4 and 5 qubits are utilized, encompassing arbitrary states, partial differential equation (PDE) states, quantum machine learning (QML) states, and quantum error correction (QEC) codewords. Arbitrary states are generated following the uniform (Haar)

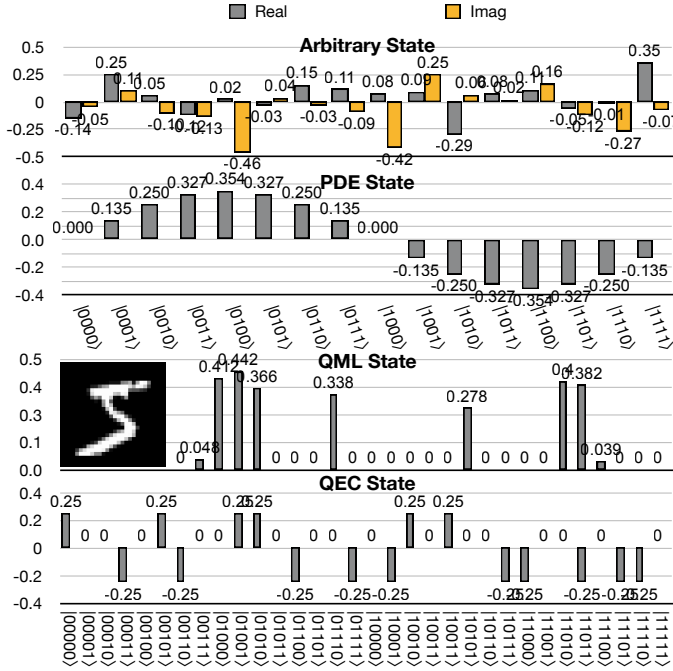


Fig. 9. Visualization of several target states. The y axis represents the amplitude on a specific basis.

measure. PDE states are real-valued states encoded into the amplitude of the basis states that are of interest to studying solving PDE by a variational quantum algorithm, such as the sine wave and the Gaussian distribution. The QML state encodes a classical MNIST hand-writing digit image [44] into the state vector via amplitude encoding [69], with the image being down-sampled, flattened, and normalized as the state. For the 5-qubit scenario, quantum error correction (QEC) codewords for the 5-qubit error correction code are also tested [41]. Fig. 9 displays the amplitude distributions of several chosen states. Additional variational quantum algorithms, such as unitary synthesis and quantum state regression, are examined as well. Quantum state regression can be considered a model for quantum metrology [60].

**Ansatz design.** The first step of variational methods is ansatz design. Fig. 10 shows the designs of our hardware-efficient ansatz. The basic unit of the ansatz is a 2-Q block shown in Fig. 10(a), inspired by [58]. In our experiments, we use the RZX gate as the 2-Q entangling gate on IBM machines that support pulse controls and CNOT gate on other IBM quantum machines. The blocks are only applied on neighboring qubits with direct connections to avoid any additional compilation overhead such as SWAP insertions.

**Pulse gate setups.** To generate  $RZX(\theta)$  gates, we use Qiskit’s `RZXCalibrationBuilder` and implement our own `RXCalibrationBuilder` accordingly for  $RX(\theta)$  gates. In addition to these two additional transpiling arguments, we also specify the virtual to physical qubit mapping, so our topology-aware ansatzes will work as expected. All the other options are set to Qiskit’s default.

**Training setups.** We use Adam optimizer with learning rate

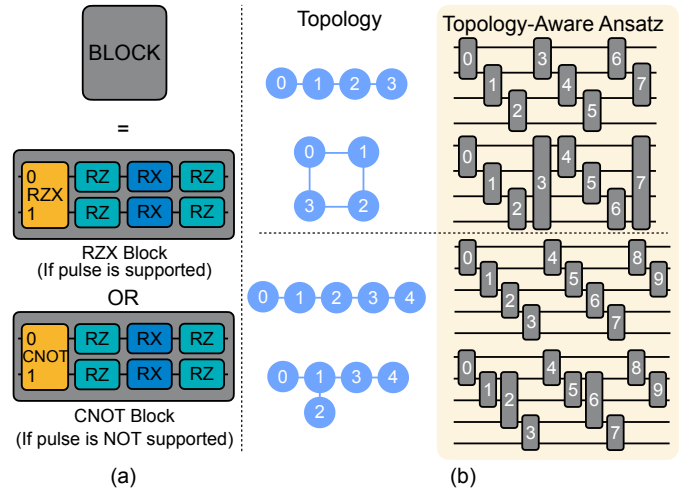


Fig. 10. (a) The basic 2-Q block used in the hardware efficient ansatz. The 2-Q gates and 1-Q gates are chosen based on the native gates of the given hardware. (b) The proposed topology-aware ansatz design with RZX or CNOT as entangling gates. The topology-aware ansatz acts only on qubits with direct connections and attempts to execute as many blocks simultaneously as possible.

$5 \times 10^{-3}$ . The loss function is  $\sqrt{\text{tr}((\rho - \hat{\rho})^2)}$ , where  $\rho$  is the target density matrix and  $\hat{\rho}$  is state generated from the ansatz. We train the ansatz for a total of 550 steps. For the first 500 steps,  $\hat{\rho}$  is obtained from a classical simulator, so the training is noise unaware; for the last 50 steps, the training is noise aware, and  $\hat{\rho}$  is obtained from the tomography results.

**Tomography setups.** Unless otherwise stated, we use classical shadow tomography with all the bases measured to improve the accuracy of tomography. That is  $3^4$  bases for 4-Q states and  $3^5$  bases for 5-Q states. For each basis, we repeat for 1024 shots. Due to limited shots, the estimated fidelity has a standard deviation of about 0.006, according to our simulation results.

## B. Experiment Results

**Variational v.s. Arithmetic.** As a baseline, we compare RobustState to the `initialize` method provided by Qiskit [1], which is the only integrated arbitrary state preparation method in the Qiskit library. The `initialize` function in Qiskit is implemented based on an analog of Quantum Shannon Decomposition [79]. We transpile the state preparation circuits generated by both methods with the highest `optimization_level=3`.

Fig. 11 shows the measured state preparation fidelity of RobustState on 3 kinds of states and 6 quantum machines with no pulse supports for 4 qubits and 5 qubits, respectively. Arithmetic decomposition tests the Qiskit baseline; Noise-unaware VQSP tests the classically trained VQSP, and RobustState is trained with real machine noise. For the tested 4-Q states, RobustState can achieve 83% fidelity and a 50% improvement on average over the Qiskit baseline.

The improvement is even more significant for 5 qubits. The Qiskit baseline averages at 5% fidelity while RobustState achieved 77% fidelity – a 72% improvement over the Qiskit baseline. These results demonstrate that, as we speculated in

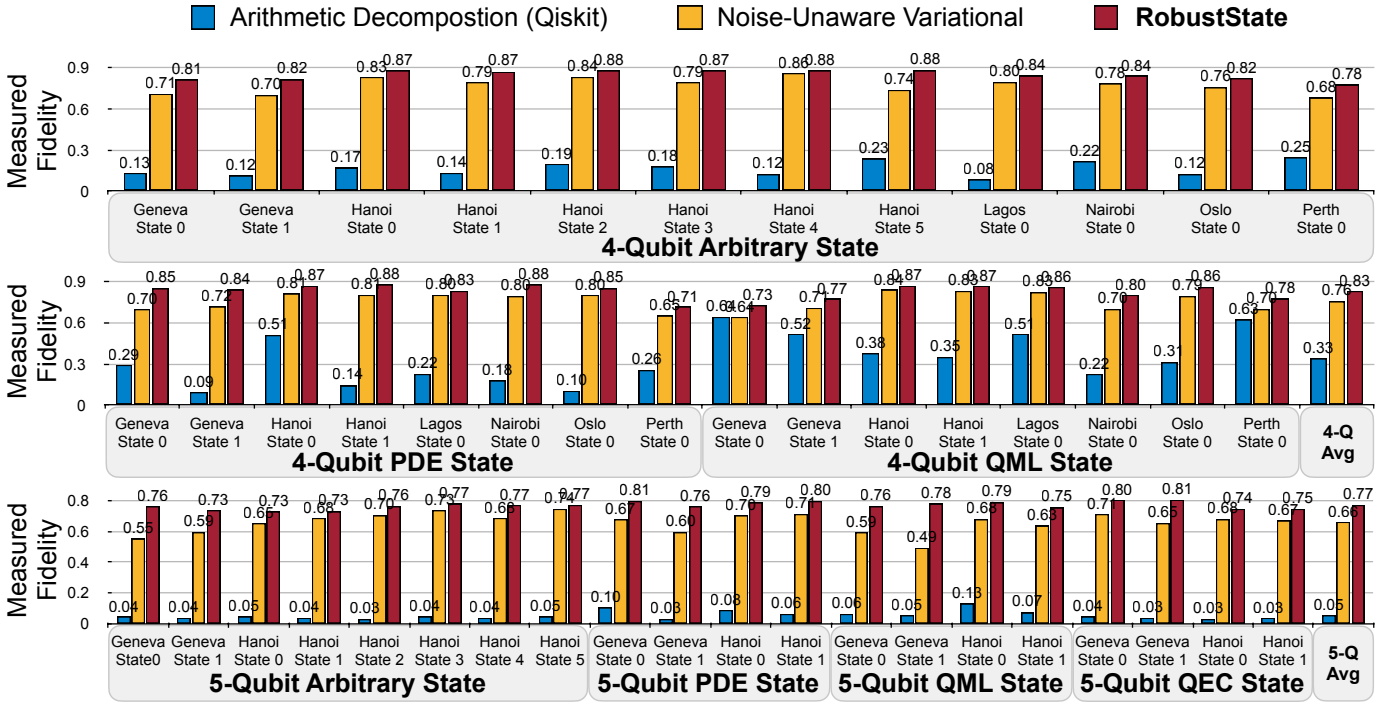


Fig. 11. RobustState using topology-aware ansatz with CNOT gates achieves the highest fidelity on various real machines for a number 4-Q target states when compared with the Qiskit baseline. Evaluated on real machines.

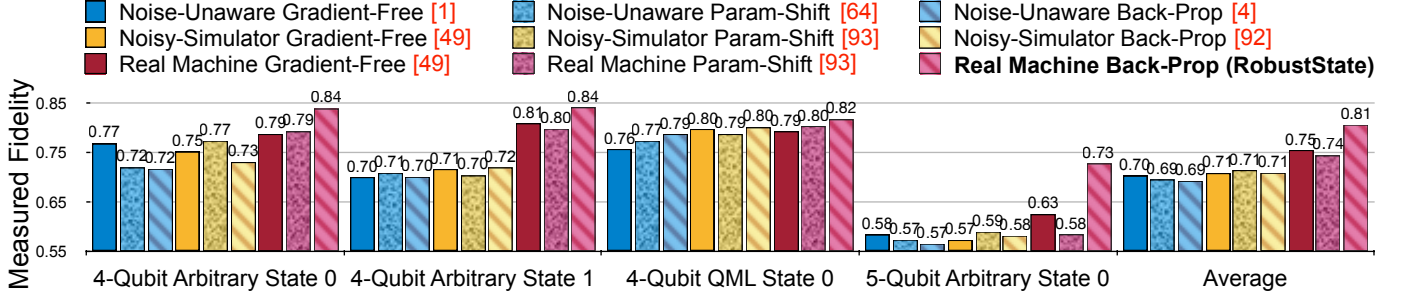


Fig. 12. RobustState compared with eight other variational state preparation methods. RobustState achieved the highest fidelity for all four tasks. Evaluated on real machines.

previous sections, VQSP algorithms perform much better than AD ones on NISQ. Moreover, RobustState can further improve the fidelity achieved by conventional VQSP.

**Additional arithmetic decomposition algorithm and error mitigation.** We perform additional baseline tests with the Mottonen algorithm [66] implemented by PennyLane [4] as an alternative baseline algorithm to the Qiskit baseline, as well as SWAP-based Bidirectional (SABRE) heuristic search algorithm [45] included by the Qiskit library used to optimize the qubit mapping to reduce SWAP gate count. SABRE was implemented on both the Qiskit baseline and the Mottonen baseline. As shown in Table III, RobustState outperforms Mottonen and Qiskit on average by 53.6% and 42.5% respectively. Even after applying SABRE, RobustState still outperforms Mottonen and Qiskit on average by 47.0% and 35.1%, respectively.

**Comparison to other optimization methods.** As introduced

Fidelity	Arbitrary	PDE	QML	Avg.
Mottonen [4], [66]	0.156	0.175	0.269	0.200
Mottonen+SABRE [4], [45], [66]	0.099	0.401	0.299	0.266
Qiskit [36]	0.176	0.277	0.481	0.311
Qiskit + SABRE [45]	0.262	0.266	0.626	0.385
<b>Ours</b>	<b>0.777</b>	<b>0.713</b>	<b>0.718</b>	<b>0.736</b>

TABLE III

ROBUSTSTATE CAN OUT-PERFORM ARITHMETIC DECOMPOSITION METHODS EVEN WHEN NOISE MITIGATION TECHNIQUE SUCH AS SABRE IS APPLIED.

in Fig. 1, we compare RobustState with all eight other optimization methods. We choose the state-of-the-art optimizer, the Nelder-Mead method provided by scipy with the default setting [22] for gradient-free optimizations, and for parameter shift, we choose the learning rate to be  $5e-3$ . As shown in Fig. 12, RobustState achieves the highest fidelity for all



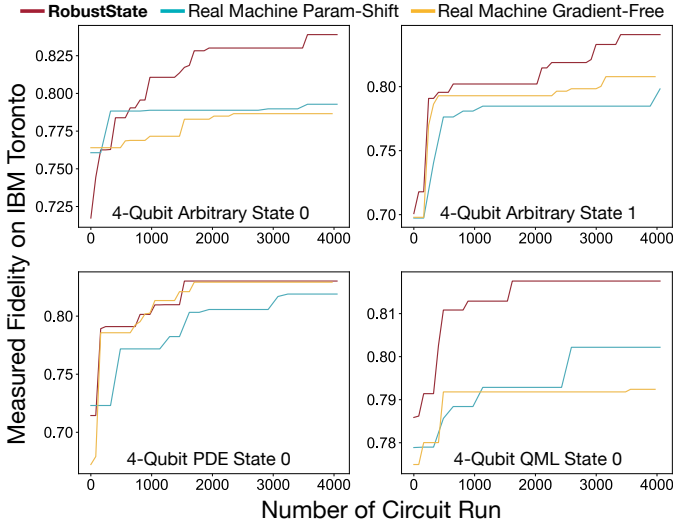


Fig. 13. Comparison of three different optimization methods. Among them, RobustState performs the best.

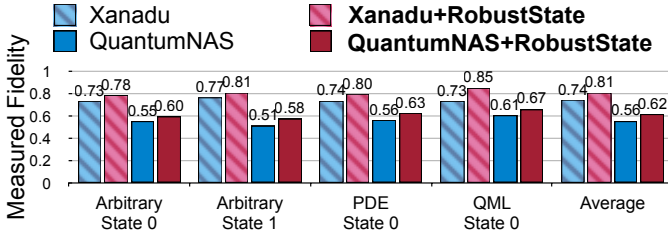


Fig. 14. RobustState can be combined with existing ansatzes and improve their fidelity.

four tasks tested and outperforms the second-best variational approach by 6% on average. This result shows that, with the highest training efficiency and noise-robustness, RobustState is better than all other variational state preparation.

We then show the training curves of RobustState, parameter shift optimization and gradient-free optimization on real machines in Fig. 13, since these are the two methods trained using real machines. For a fair comparison, we show the fidelity improvement w.r.t. the number of circuit executions. As Fig. 13 shows, our optimization method outperforms gradient-free optimization in 3 out of 4 tasks, and have equaling performance for the last task, and outperforms parameter shift in all the four tasks.

**Applicability to other ansatzes.** As a framework for state preparation problems, we use Fig. 14 to show that RobustState is applicable to other variational ansatzes. We apply RobustState on the ansatzes proposed in QuantumNAS [91] and by Xanadu [2]. In the QuantumNAS ansatz, each block contains 8 layers, the gate count of each layer is [2, 2, 4, 4, 1, 2, 2, 1], and gate type is RX, RY, RZ, CNOT, RX, RY, RZ, CNOT, respectively. We use 4 blocks to ensure convergence. The Xanadu ansatz is originally designed for photonic quantum computers, so we adopt the design philosophy of the ansatz and implement it on superconducting quantum computers. Each block of the ansatz consists of one layer of neighboring CNOT

	Pulse	Gate	RobustState+Pulse
Low Coherent Error	✗	✓	✓
Low Incoherent Errors	✓	✗	✓

TABLE IV

ROBUSTSTATE HAS THE UNIQUE ADVANTAGES OF BOTH LOW COHERENT AND INCOHERENT ERRORS WHEN COMBINED WITH PULSE LEVEL ANSATZ.

Task	Baseline	Ours
Unitary Synthesis Jakarta	0.845	<b>0.868</b>
Unitary Synthesis Toronto	0.858	<b>0.940</b>
Unitary Synthesis Perth (1)	0.817	<b>0.834</b>
Unitary Synthesis Perth (2)	0.798	<b>0.821</b>
Quantum State Regression (1) Loss	0.167	<b>0.147</b>
Quantum State Regression (2) Loss	0.163	<b>0.124</b>

TABLE V

PERFORMANCE OF ROBUSTSTATE ON OTHER VARIATIONAL TASKS.

gates as the entangling layer, one layer of single-qubit rotations, then another entangling layer, and two more layers of single-qubit rotations. We use 3 blocks to ensure convergence. As shown in Fig. 14, on average RobustState improves the fidelity of the Xanadu ansatz and QuantumNAS ansatz by 7% and 6%, with a final fidelity of 81% and 62%, respectively.

**Pulse ansatz.** Fig. 15 shows the RobustState performance for 4-Q states and 5-Q states on three machines with pulse supports using RZX blocks. We use Qiskit as our baseline here as well. RobustState on pulse level VQSP improves the average fidelity by 8% and 10% for 4-Q and 5-Q, producing final fidelities of 79% and 61%, respectively. Furthermore, RobustState with pulse outperforms the baseline by 42% and 57% for 4-Q and 5-Q, respectively.

An interesting phenomenon is that sometimes the noise-free trained circuit compiled to non-native basis gates performs better than that compiled to native pulse gates. This might be caused by the additional coherent error introduced by tuning pulses. Nevertheless, pulse ansatz enables *better optimization space* so the final fidelity can be higher. Fig. 16 shows the fidelity of noise-aware training with gate ansatz v.s. with pulse ansatz for two arbitrary states on the IBMQ Montreal machine. We can clearly see that the fidelity of the pulse ansatz surpasses the non-native gates in the middle of training. This shows that by combining pulse ansatz and the noise-aware gradients together, we can reduce both coherent and incoherent errors to achieve the best fidelity of quantum states, as illustrated in Table IV.

**Results on other variational tasks.** RobustState is generally applicable to many other variational tasks. As an example, we test our method with quantum state regression and unitary synthesis. The quantum state regression takes an input state  $\cos(\theta)|000\rangle + e^{i\phi}\sin(\theta)|111\rangle$  and predicts the values  $\sin(2\theta)\cos(\phi)$  for task 1 and  $\sin(2\theta)\sin(\phi)$  for task 2. The ansatz also follows from QuantumNAS [91]. Our method can further reduce the loss for 0.03 compared to noise-unaware training (baseline), as shown in Table V.

For unitary synthesis, we test our method for 2-Q random unitary. The ansatz we use is 6 layers of RZX + arbitrary 1-

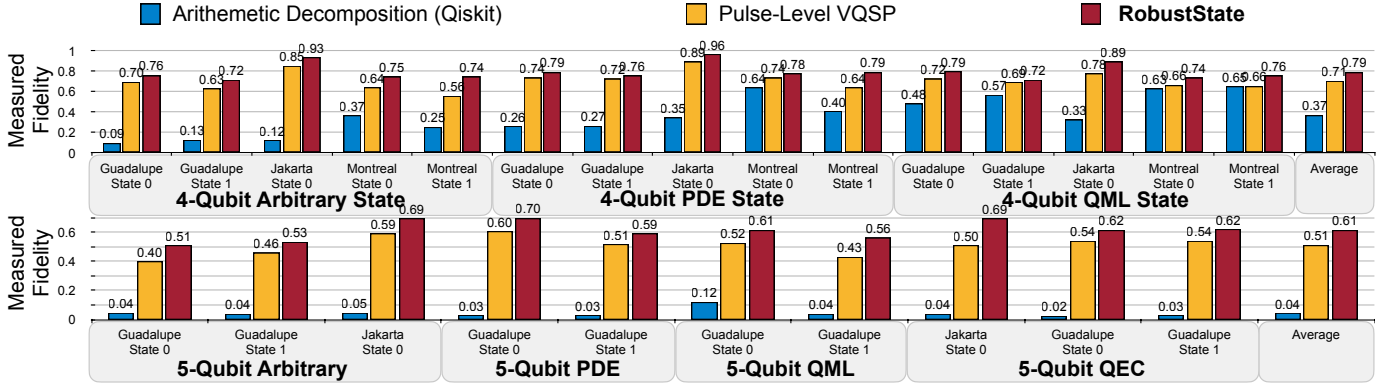


Fig. 15. On three machines, IBMQ Guadalupé, IBMQ Jakarta, and IBMQ Montréal, with pulse supports, RobustState using the topology-aware ansatz with RZX gates achieves the highest fidelity for various 4-Q states when compared with the Qiskit baseline. Evaluated on real machines.

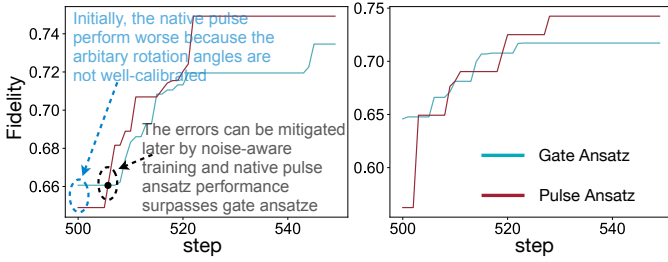


Fig. 16. Training curves for the last 50 steps with the noise-aware loss for hardware-efficient ansatz using native pulse and hardware-efficient ansatz using the non-native CNOT gates. The first 500 steps are not included since they only use classical noise-free training.

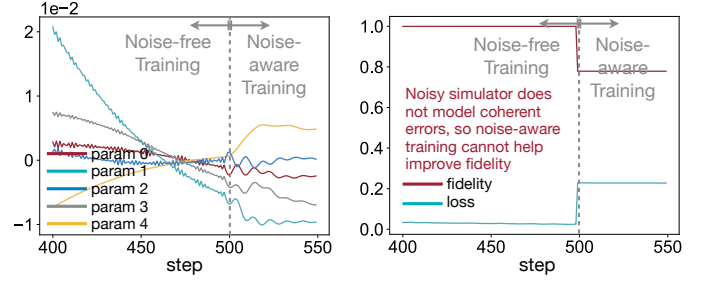


Fig. 18. Training curves for selected parameters of an experiment on a noisy simulator (left); Evolution of state fidelity and loss value on the same experiment (right). The dashed lines at step 500 mark the transition from noise-free training to noise-aware training.

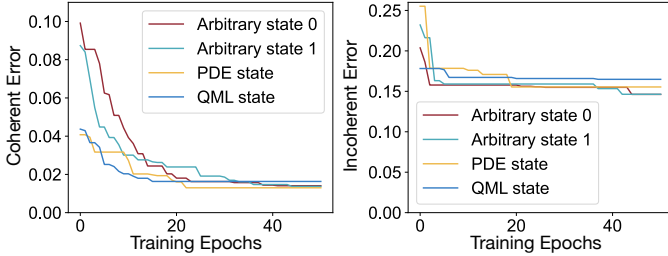


Fig. 17. The coherent and incoherent errors of four state preparation tasks. Our noise-aware training method significantly reduces coherent errors.

Q gates. Compared to noise-unaware training (baseline), our method can improve the fidelity of unitaries for 3.6%.

### C. Result Analysis

**Where does our advantage come from?** The noise-aware training part of our framework is targeted to eliminate coherent errors by fine-tuning the parameters. To show this, we separate the coherent error from the incoherent error in Fig. 17. For the four states, our method can reduce the coherent errors by at least 62% and up to 86%. However, for incoherent error, it is only reduced by as low as 7% and no more than 39%.

This can be further illustrated with a simulator experiment. We conduct our method with similar settings but on a noisy simulator instead of real quantum computers. As shown in Fig. 18, the parameters do not change substantially when

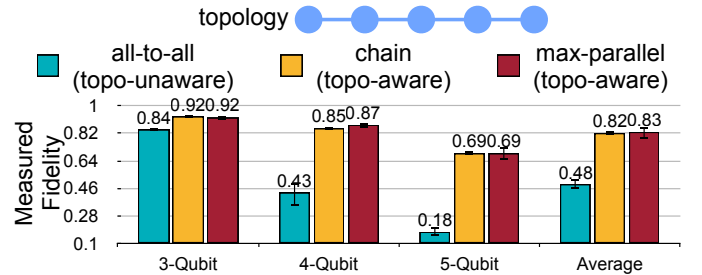


Fig. 19. The topology-aware ansatz compared with the topology-unaware ansatz with classically optimized parameters run on a linear array of qubits of IBM Hanoi.

training with noise-aware gradients, and the fidelity is only marginally improved. This is not surprising, as the Qiskit noisy simulator only models incoherent errors (This is not to say that the simulator cannot simulate coherent error, but that the current noise model used by the noisy simulator has insufficient information about coherent errors. During calibration, if we find an over-rotation error, we will immediately fix the error by reducing the pulse amplitude instead of writing that information into the noise model). Noise-aware gradient, by itself, does not change the circuit depth, so it cannot optimize the parameters for a simulator without any coherent error.

**Whether the topology-aware ansatzes perform better?** In

Topology	Noise-Unaware Back-Prop	RobustState
I	0.828	<b>0.875</b>
T	0.674	<b>0.797</b>

TABLE VI  
FIDELITY FOR DIFFERENT TOPOLOGIES

the noise-free simulation of different ansatzes, both topology-aware and topology-unaware ansatzes converge to the target state with a similar number of *blocks*. We show the results of running these state preparation circuits on a set of linearly connected qubits from the IBM Hanoi machine in Fig. 19 using 3, 4, and 5 qubits. The fidelities dropped from 3 to 5 qubits as the deeper circuits would introduce more noise. For the topology-aware ansatz, fidelity went from 92% to 69%, while for the topology-unaware ansatz, the fidelity went from 84% to 18%, showing importance of topology awareness.

#### Whether our method generalizes to different topologies?

We test our method with different topology (Table VI), the *I* type (the first row of Fig. 10) and *T* type (the last row of Fig. 10). Both of them use the topology-aware ansatz. It can be seen from the table that our method works well for different topologies. And for the topology-aware ansatz, the *I* topology works better since it has a shallower circuit.

**Is our method scalable?** Preparing small-to-medium states with high fidelity is essential to many quantum algorithms in the NISQ era. For problems with small sizes, the cost of the noise-free training part is negligible. On a Mac with M1-pro processor and the TorchQuantum library [91], training for 500 steps takes about 6.02s for a 4-Q ansatz with 12 CNOT *blocks*, and 11.12s for a 5-Q ansatz with 20 CNOT *blocks*. TorchQuantum supports training for up to 30 qubits, so classical simulation is not a problem for medium-sized tasks. With regards to on-chip training, the classical shadow tomography we used enables us to update the parameter in a stochastic way which can mitigate the scaling issue. We sample 40 bases out of 81 bases to estimate the loss function, and our experiments show that basis sampling enables faster convergence and higher fidelity. The results are shown in Fig. 20. Though our method cannot scale up with even more qubits, preparing quantum states with a few qubits with high fidelity is already very useful for near-term NISQ and long-term fault-tolerant quantum computing.

## V. RELATED WORK

### A. Pulse-Level Quantum Computing

Recently, quantum algorithm optimization on the pulse signal level has attracted increasing research interest [10], [16], [23], [37], [49], [62], [80]. A series of works explores Quantum Optimal Control [10], [16], [80], which iteratively optimizes the pulse shapes of channels of the systems by minimizing the distance between the computed Unitary matrix of the pulses and the target. Another research focus is on variational pulse learning [37], [48], [49], [62] in which pulse shape parameters (such as amplitude, frequency, and duration) are directly optimized instead of the angles of rotation gates. [23]

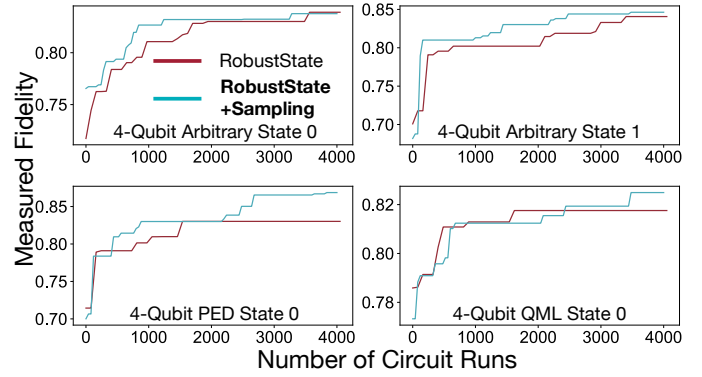


Fig. 20. Comparison between full state tomography and basis sampling. Basis sampling works better than full tomography in general.

proposes to compile the gates to the native gate sets to reduce the circuit depth. Our method improves upon theirs because our hybrid training can mitigate the unwanted coherent errors introduced by directly changing pulse shapes according to gate parameters.

### B. Noise-Aware Quantum Compilation

Noise constitutes a significant challenge in NISQ machines, prompting the development of various noise-adaptive quantum compilation techniques to mitigate its effects [15], [70], [76], [85], [94], [95], [96], [97]. These approaches aim to reduce noise impact by addressing diverse gate errors that can be suppressed through different strategies. Qubit mapping techniques [45], [53], [65], [67], [86], [105] help minimize noise by optimizing the assignment of logical qubits to physical qubits on quantum devices. Composite pulses [7], [55], [63], [102] involve designing sequences of pulses that achieve a desired operation while mitigating errors caused by noise. Dynamical decoupling [6], [14], [29], [51], [89] techniques are employed to isolate quantum systems from their environment, reducing the impact of noise on their evolution. Randomized compiling [90] introduces randomness into quantum circuits to average out systematic errors, while hidden inverses [104] utilize a set of quantum operations that are robust against specific noise channels. Instruction scheduling [68], [101] optimizes the order of quantum operations to minimize noise, and frequency tuning [18], [30], [88] adjusts the frequencies of qubits to reduce crosstalk and enhance gate fidelity. Parallel execution on multiple machines [83] leverages the resources of several quantum devices to overcome noise limitations. Algorithm-aware design and compilation techniques [11], [43], [47], [107] tailor the compilation process to exploit specific algorithmic properties, leading to improved noise resilience. Finally, qubit-specific basis gate approaches [46], [52] design custom basis gates for individual qubits, optimizing their performance in the presence of noise.

## VI. CONCLUSION

We introduce RobustState, a noise-aware training framework for robust quantum state preparation. Our framework's key feature is its ability to combine noise-impacted outputs from

real machines and intermediate results from simulators to perform noise-aware back-propagation. This approach results in highly noise-robust parameters and increased training efficiency. We thoroughly evaluate the RobustState framework on 10 real quantum machines, showcasing a reduction of over  $7.1\times$  in coherent error and achieving, on average, 50% and 72% fidelity improvements over baselines. We also validate our noise-aware training on other variational algorithms including unitary synthesis and state regression. Moving forward, we anticipate that the proposed noise-aware training framework can be generalized to other variational algorithms to mitigate real machine noise and serve as a valuable subroutine for numerous quantum algorithms.

## REFERENCES

- [1] M. S. ANIS *et al.*, “Qiskit: An open-source framework for quantum computing,” 2021.
- [2] J. M. Arrazola, T. R. Bromley, J. Izaac, C. R. Myers, K. Brádler, and N. Killoran, “Machine learning method for state preparation and gate synthesis on photonic quantum computers,” *Quantum Science and Technology*, vol. 4, no. 2, p. 024004, 2019.
- [3] C. W. Bauer, P. Deliyannis, M. Freytsis, and B. Nachman, “Practical considerations for the preparation of multivariate gaussian states on quantum computers,” 2021. [Online]. Available: <https://arxiv.org/abs/2109.10918>
- [4] V. Bergholm, J. Izaac, M. Schuld, C. Gogolin, M. S. Alam, S. Ahmed, J. M. Arrazola, C. Blank, A. Delgado, and S. Jahangiri, “PennyLane: Automatic differentiation of hybrid quantum-classical computations,” *arXiv preprint arXiv:1811.04968*, 2018.
- [5] J. Biamonte, P. Wittek, N. Pancotti, P. Rebentrost, N. Wiebe, and S. Lloyd, “Quantum machine learning,” *Nature*, vol. 549, no. 7671, pp. 195–202, 2017.
- [6] M. J. Biercuk, H. Uys, A. P. VanDevender, N. Shiga, W. M. Itano, and J. J. Bollinger, “Optimized dynamical decoupling in a model quantum memory,” *Nature*, vol. 458, no. 7241, pp. 996–1000, 2009.
- [7] K. R. Brown, A. W. Harrow, and I. L. Chuang, “Arbitrarily accurate composite pulse sequences,” *Physical Review A*, vol. 70, no. 5, p. 052318, 2004.
- [8] C. D. Bruzewicz, J. Chiaverini, R. McConnell, and J. M. Sage, “Trapped-ion quantum computing: Progress and challenges,” *Applied Physics Reviews*, vol. 6, no. 2, p. 021314, 2019.
- [9] I. Byun, J. Kim, D. Min, I. Nagaoka, K. Fukumitsu, I. Ishikawa, T. Tanimoto, M. Tanaka, K. Inoue, and J. Kim, “Xqsim: Modeling cross-technology control processors for 10+k qubit quantum computers,” in *Proceedings of the 49th Annual International Symposium on Computer Architecture*, ser. ISCA ’22. New York, NY, USA: Association for Computing Machinery, 2022, p. 366–382. [Online]. Available: <https://doi.org/10.1145/3470496.3527417>
- [10] J. Cheng, H. Deng, and X. Qia, “Accqoc: Accelerating quantum optimal control based pulse generation,” in *2020 ACM/IEEE 47th Annual International Symposium on Computer Architecture (ISCA)*. IEEE, 2020, pp. 543–555.
- [11] J. Cheng, H. Wang, Z. Liang, Y. Shi, S. Han, and X. Qian, “Topgen: Topology-aware bottom-up generator for variational quantum circuits,” *arXiv preprint arXiv:2210.08190*, 2022.
- [12] L. Cincio, K. Rudinger, M. Sarovar, and P. J. Coles, “Machine learning of noise-resilient quantum circuits,” *PRX Quantum*, vol. 2, no. 1, p. 010324, 2021.
- [13] P. Das, C. A. Pattison, S. Manne, D. M. Carmean, K. M. Svore, M. Qureshi, and N. Delfosse, “Afs: Accurate, fast, and scalable error-decoding for fault-tolerant quantum computers,” in *2022 IEEE International Symposium on High-Performance Computer Architecture (HPCA)*. IEEE, 2022, pp. 259–273.
- [14] P. Das, S. Tannu, S. Dangwal, and M. Qureshi, “Adapt: Mitigating idling errors in qubits via adaptive dynamical decoupling,” in *MICRO-54: 54th Annual IEEE/ACM International Symposium on Microarchitecture*, 2021, pp. 950–962.
- [15] P. Das, S. Tannu, and M. Qureshi, “Jigsaw: Boosting fidelity of nisy programs via measurement subsetting,” in *MICRO-54: 54th Annual IEEE/ACM International Symposium on Microarchitecture*, 2021, pp. 937–949.
- [16] R. de Keijzer, O. Tse, and S. Kokkelsmans, “Pulse based variational quantum optimal control for hybrid quantum computing,” *arXiv preprint arXiv:2202.08908*, 2022.
- [17] D. Dieks, “Communication by epr devices,” *Physics Letters A*, vol. 92, no. 6, pp. 271–272, 1982.
- [18] Y. Ding, P. Gokhale, S. F. Lin, R. Rines, T. Propson, and F. T. Chong, “Systematic crosstalk mitigation for superconducting qubits via frequency-aware compilation,” in *2020 53rd Annual IEEE/ACM International Symposium on Microarchitecture (MICRO)*. IEEE, 2020, pp. 201–214.
- [19] E. Farhi, J. Goldstone, and S. Gutmann, “A quantum approximate optimization algorithm,” *arXiv preprint arXiv:1411.4028*, 2014.
- [20] A. G. Fowler, M. Mariantoni, J. M. Martinis, and A. N. Cleland, “Surface codes: Towards practical large-scale quantum computation,” *Physical Review A*, vol. 86, no. 3, p. 032324, 2012.
- [21] J. M. Gambetta, F. Motzoi, S. Merkel, and F. K. Wilhelm, “Analytic control methods for high-fidelity unitary operations in a weakly nonlinear oscillator,” *Physical Review A*, vol. 83, no. 1, p. 012308, 2011.
- [22] F. Gao and L. Han, “Implementing the nelder-mead simplex algorithm with adaptive parameters,” *Computational Optimization and Applications*, vol. 51, no. 1, pp. 259–277, 2012.
- [23] P. Gokhale, A. Javadi-Abhari, N. Earnest, Y. Shi, and F. T. Chong, “Optimized quantum compilation for near-term algorithms with open-pulse,” in *2020 53rd Annual IEEE/ACM International Symposium on Microarchitecture (MICRO)*. IEEE, 2020, pp. 186–200.
- [24] P. Gokhale, A. Javadi-Abhari, N. Earnest, Y. Shi, and F. T. Chong, “Optimized quantum compilation for near-term algorithms with open-pulse,” in *2020 53rd Annual IEEE/ACM International Symposium on Microarchitecture (MICRO)*, 2020, pp. 186–200.
- [25] J. Gonzalez-Conde, Ángel Rodríguez-Rozas, E. Solano, and M. Sanz, “Simulating option price dynamics with exponential quantum speedup,” 2022.
- [26] D. Gottesman, “An introduction to quantum error correction and fault-tolerant quantum computation,” in *Quantum information science and its contributions to mathematics, Proceedings of Symposia in Applied Mathematics*, vol. 68, 2010, pp. 13–58.
- [27] L. Grover and T. Rudolph, “Creating superpositions that correspond to efficiently integrable probability distributions,” *arXiv e-prints*, pp. quant-ph/0208112, Aug. 2002.
- [28] L. K. Grover, “A fast quantum mechanical algorithm for database search,” in *Proceedings of the twenty-eighth annual ACM symposium on Theory of computing*, 1996, pp. 212–219.
- [29] E. L. Hahn, “Spin echoes,” *Physical review*, vol. 80, no. 4, p. 580, 1950.
- [30] F. Helmer, M. Mariantoni, A. G. Fowler, J. von Delft, E. Solano, and F. Marquardt, “Cavity grid for scalable quantum computation with superconducting circuits,” *EPL (Europhysics Letters)*, vol. 85, no. 5, p. 50007, 2009.
- [31] A. Holmes and A. Y. Matsuura, “Efficient quantum circuits for accurate state preparation of smooth, differentiable functions,” 2020. [Online]. Available: <https://arxiv.org/abs/2005.04351>
- [32] C. Horsman, A. G. Fowler, S. Devitt, and R. Van Meter, “Surface code quantum computing by lattice surgery,” *New Journal of Physics*, vol. 14, no. 12, p. 123011, 2012.
- [33] J. Hsu, “Ces 2018: Intel’s 49-qubit chip shoots for quantum supremacy,” <https://spectrum.ieee.org/tech-talk/computing/hardware/intels-49qubit-chip-aims-for-quantum-supremacy>.
- [34] H.-Y. Huang, R. Kueng, and J. Preskill, “Predicting many properties of a quantum system from very few measurements,” *Nature Physics*, vol. 16, no. 10, pp. 1050–1057, 2020.
- [35] IBM, “Ibm unveils 400 qubit-plus quantum processor and next-generation ibm quantum system two,” <https://newsroom.ibm.com/2022-11-09-IBM-Unveils-400-Qubit-Plus-Quantum-Processor-and-Next-Generation-IBM-Quantum-System-Two>.
- [36] Q. IBM, Apr 2021. [Online]. Available: <https://qiskit.org/textbook/ch-quantum-hardware/calibrating-qubits-pulse.html>
- [37] J. R. Johansson, P. D. Nation, and F. Nori, “Qutip: An open-source python framework for the dynamics of open quantum systems,” *Computer Physics Communications*, vol. 183, no. 8, pp. 1760–1772, 2012.



- [38] A. Kandala, A. Mezzacapo, K. Temme, M. Takita, M. Brink, J. M. Chow, and J. M. Gambetta, "Hardware-efficient variational quantum eigensolver for small molecules and quantum magnets," *Nature*, vol. 549, no. 7671, pp. 242–246, 2017.
- [39] J. Kelly, "A preview of bristlecone, google's new quantum processor," <https://ai.googleblog.com/2018/03/a-preview-of-bristlecone-googles-new.html>.
- [40] A. Kitaev and W. A. Webb, "Wavefunction preparation and resampling using a quantum computer," 2008. [Online]. Available: <https://arxiv.org/abs/0801.0342>
- [41] E. Knill, R. Laflamme, R. Martinez, and C. Negrevergne, "Benchmarking quantum computers: The five-qubit error correcting code," *Physical Review Letters*, vol. 86, no. 25, p. 5811, 2001.
- [42] P. Krantz, M. Kjaergaard, F. Yan, T. P. Orlando, S. Gustavsson, and W. D. Oliver, "A quantum engineer's guide to superconducting qubits," *Applied Physics Reviews*, vol. 6, no. 2, p. 021318, 2019.
- [43] L. Lao and D. E. Browne, "2qan: A quantum compiler for 2-local qubit hamiltonian simulation algorithms," in *Proceedings of the 49th Annual International Symposium on Computer Architecture*, 2022, pp. 351–365.
- [44] Y. Lecun, L. Bottou, Y. Bengio, and P. Haffner, "Gradient-based learning applied to document recognition," *Proceedings of the IEEE*, vol. 86, no. 11, pp. 2278–2324, 1998.
- [45] G. Li, Y. Ding, and Y. Xie, "Tackling the qubit mapping problem for nisq-era quantum devices," in *Proceedings of the Twenty-Fourth International Conference on Architectural Support for Programming Languages and Operating Systems*, 2019, pp. 1001–1014.
- [46] G. Li, Y. Shi, and A. Javadi-Abhari, "Software-hardware co-optimization for computational chemistry on superconducting quantum processors," in *2021 ACM/IEEE 48th Annual International Symposium on Computer Architecture (ISCA)*. IEEE, 2021, pp. 832–845.
- [47] G. Li, A. Wu, Y. Shi, A. Javadi-Abhari, Y. Ding, and Y. Xie, "Paulihedral: a generalized block-wise compiler optimization framework for quantum simulation kernels," in *Proceedings of the 27th ACM International Conference on Architectural Support for Programming Languages and Operating Systems*, 2022, pp. 554–569.
- [48] Z. Liang, J. Cheng, H. Ren, H. Wang, F. Hua, Y. Ding, F. Chong, S. Han, Y. Shi, and X. Qian, "Pan: Pulse ansatz on nisq machines," *arXiv preprint arXiv:2208.01215*, 2022.
- [49] Z. Liang\*, H. Wang\*, J. Cheng, Y. Ding, H. Ren, Z. Gao, Z. Hu, D. S. Boning, X. Qian, S. Han et al., "Variational quantum pulse learning," in *2022 IEEE International Conference on Quantum Computing and Engineering (QCE)*. IEEE, 2022, pp. 556–565.
- [50] Z. Liang, Z. Wang, J. Yang, L. Yang, Y. Shi, and W. Jiang, "Can noise on qubits be learned in quantum neural network? a case study on quantumflow," in *2021 IEEE/ACM International Conference On Computer Aided Design (ICCAD)*. IEEE, 2021, pp. 1–7.
- [51] D. A. Lidar, "Review of decoherence free subspaces, noiseless sub-systems, and dynamical decoupling," *Adv. Chem. Phys.*, vol. 154, pp. 295–354, 2014.
- [52] S. F. Lin, S. Sussman, C. Duckering, P. S. Mundada, J. M. Baker, R. S. Kumar, A. A. Houck, and F. T. Chong, "Let each quantum bit choose its basis gates," *arXiv preprint arXiv:2208.13380*, 2022.
- [53] L. Liu and X. Dou, "Qucloud: A new qubit mapping mechanism for multi-programming quantum computing in cloud environment," in *2021 IEEE International Symposium on High-Performance Computer Architecture (HPCA)*, 2021, pp. 167–178.
- [54] S. Lloyd, M. Mohseni, and P. Rebentrost, "Quantum algorithms for supervised and unsupervised machine learning," *arXiv preprint arXiv:1307.0411*, 2013.
- [55] G. H. Low, T. J. Yoder, and I. L. Chuang, "Optimal arbitrarily accurate composite pulse sequences," *Physical Review A*, vol. 89, no. 2, p. 022341, 2014.
- [56] M. Lubasch, J. Joo, P. Moinier, M. Kiffner, and D. Jaksch, "Variational quantum algorithms for nonlinear problems," *Physical Review A*, vol. 101, no. 1, jan 2020. [Online]. Available: <https://doi.org/10.1103/PhysRevA.101.010301>
- [57] F. B. Maciejewski, Z. Zimborás, and M. Oszmaniec, "Mitigation of readout noise in near-term quantum devices by classical post-processing based on detector tomography," *Quantum*, vol. 4, p. 257, 2020.
- [58] L. Madden and A. Simonetto, "Best approximate quantum compiling problems," *ACM Transactions on Quantum Computing*, vol. 3, no. 2, mar 2022. [Online]. Available: <https://doi.org/10.1145/3505181>
- [59] E. Magesan, J. M. Gambetta, and J. Emerson, "Characterizing quantum gates via randomized benchmarking," *Physical Review A*, vol. 85, no. 4, p. 042311, 2012.
- [60] C. D. Marciniak, T. Feldker, I. Pogorelov, R. Kaubruegger, D. V. Vasilyev, R. van Bijnen, P. Schindler, P. Zoller, R. Blatt, and T. Monz, "Optimal metrology with programmable quantum sensors," *Nature*, vol. 603, no. 7902, pp. 604–609, 2022.
- [61] G. Marin-Sanchez, J. Gonzalez-Conde, and M. Sanz, "Quantum algorithms for approximate function loading," 2021. [Online]. Available: <https://arxiv.org/abs/2111.07933>
- [62] O. R. Meitei, B. T. Gard, G. S. Barron, D. P. Pappas, S. E. Economou, E. Barnes, and N. J. Mayhall, "Gate-free state preparation for fast variational quantum eigensolver simulations," *npj Quantum Information*, vol. 7, no. 1, pp. 1–11, 2021.
- [63] J. T. Merrill and K. R. Brown, "Progress in compensating pulse sequences for quantum computation," *Quantum Information and Computation for Chemistry*, pp. 241–294, 2014.
- [64] K. Mitarai, M. Negoro, M. Kitagawa, and K. Fujii, "Quantum circuit learning," *Physical Review A*, vol. 98, no. 3, p. 032309, 2018.
- [65] A. Molavi, A. Xu, M. Diges, L. Pick, S. Tannu, and A. Albarghouti, "Qubit mapping and routing via maxsat," *arXiv preprint arXiv:2208.13679*, 2022.
- [66] M. Mottonen, J. J. Vartiainen, V. Bergholm, and M. M. Salomaa, "Transformation of quantum states using uniformly controlled rotations," *arXiv preprint quant-ph/0407010*, 2004.
- [67] P. Murali, J. M. Baker, A. Javadi-Abhari, F. T. Chong, and M. Martonosi, "Noise-adaptive compiler mappings for noisy intermediate-scale quantum computers," in *Proceedings of the Twenty-Fourth International Conference on Architectural Support for Programming Languages and Operating Systems*, 2019, pp. 1015–1029.
- [68] P. Murali, D. C. McKay, M. Martonosi, and A. Javadi-Abhari, "Software mitigation of crosstalk on noisy intermediate-scale quantum computers," in *Proceedings of the Twenty-Fifth International Conference on Architectural Support for Programming Languages and Operating Systems*, 2020, pp. 1001–1016.
- [69] K. Nakaji, S. Uno, Y. Suzuki, R. Raymond, T. Onodera, T. Tanaka, H. Tezuka, N. Mitsuda, and N. Yamamoto, "Approximate amplitude encoding in shallow parameterized quantum circuits and its application to financial market indicators," *Physical Review Research*, vol. 4, no. 2, p. 023136, 2022.
- [70] T. Patel and D. Tiwari, "Qraft: Reverse your quantum circuit and know the correct program output," in *Proceedings of the 26th ACM International Conference on Architectural Support for Programming Languages and Operating Systems*, ser. ASPLOS '21. New York, NY, USA: Association for Computing Machinery, 2021, p. 443–455. [Online]. Available: <https://doi.org/10.1145/3445814.3446743>
- [71] A. Peruzzo, J. McClean, P. Shadbolt, M.-H. Yung, X.-Q. Zhou, P. J. Love, A. Aspuru-Guzik, and J. L. O'Brien, "A variational eigenvalue solver on a photonic quantum processor," *Nature communications*, vol. 5, no. 1, pp. 1–7, 2014.
- [72] M. Plesch and i. c. v. Brukner, "Quantum-state preparation with universal gate decompositions," *Phys. Rev. A*, vol. 83, p. 032302, Mar 2011. [Online]. Available: <https://link.aps.org/doi/10.1103/PhysRevA.83.032302>
- [73] A. G. Rattew and B. Koczor, "Preparing arbitrary continuous functions in quantum registers with logarithmic complexity," 2022. [Online]. Available: <https://arxiv.org/abs/2205.00519>
- [74] A. G. Rattew, Y. Sun, P. Minssen, and M. Pistoia, "The Efficient Preparation of Normal Distributions in Quantum Registers," *Quantum*, vol. 5, p. 609, Dec. 2021. [Online]. Available: <https://doi.org/10.22331/q-2021-12-23-609>
- [75] G. S. Ravi, J. M. Baker, A. Fayyazi, S. F. Lin, A. Javadi-Abhari, M. Pedram, and F. T. Chong, "Have your qec and bandwidth too!: A lightweight cryogenic decoder for common/trivial errors, and efficient bandwidth+ execution management otherwise," *arXiv preprint arXiv:2208.08547*, 2022.
- [76] G. S. Ravi, K. N. Smith, P. Gokhale, A. Mari, N. Earnest, A. Javadi-Abhari, and F. T. Chong, "Vaqem: A variational approach to quantum error mitigation," in *2022 IEEE International Symposium on High-Performance Computer Architecture (HPCA)*. IEEE, 2022, pp. 288–303.
- [77] P. Rebentrost, M. Mohseni, and S. Lloyd, "Quantum support vector machine for big data classification," *Physical review letters*, vol. 113, no. 13, p. 130503, 2014.

- [78] Rigetti, “Rigetti quantum,” <https://www.rigetti.com/>.
- [79] V. Shende, S. Bullock, and I. Markov, “Synthesis of quantum-logic circuits,” *IEEE Transactions on Computer-Aided Design of Integrated Circuits and Systems*, vol. 25, no. 6, pp. 1000–1010, 2006.
- [80] Y. Shi, N. Leung, P. Gokhale, Z. Rossi, D. I. Schuster, H. Hoffmann, and F. T. Chong, “Optimized compilation of aggregated instructions for realistic quantum computers,” in *Proceedings of the Twenty-Fourth International Conference on Architectural Support for Programming Languages and Operating Systems*, 2019, pp. 1031–1044.
- [81] P. W. Shor, “Polynomial-time algorithms for prime factorization and discrete logarithms on a quantum computer,” *SIAM review*, vol. 41, no. 2, pp. 303–332, 1999.
- [82] J. A. Smolin, J. M. Gambetta, and G. Smith, “Efficient method for computing the maximum-likelihood quantum state from measurements with additive gaussian noise,” *Physical review letters*, vol. 108, no. 7, p. 070502, 2012.
- [83] S. Stein, N. Wiebe, Y. Ding, P. Bo, K. Kowalski, N. Baker, J. Ang, and A. Li, “Eqc: ensembled quantum computing for variational quantum algorithms,” in *Proceedings of the 49th Annual International Symposium on Computer Architecture*, 2022, pp. 59–71.
- [84] X. Sun, G. Tian, S. Yang, P. Yuan, and S. Zhang, “Asymptotically optimal circuit depth for quantum state preparation and general unitary synthesis,” *arXiv preprint arXiv:2108.06150*, 2021.
- [85] S. Tannu, P. Das, R. Ayanzadeh, and M. Qureshi, “Hammer: Boosting fidelity of noisy quantum circuits by exploiting hamming behavior of erroneous outcomes,” in *Proceedings of the 27th ACM International Conference on Architectural Support for Programming Languages and Operating Systems*, ser. ASPLOS ’22. New York, NY, USA: Association for Computing Machinery, 2022, p. 529–540. [Online]. Available: <https://doi.org/10.1145/3503222.3507703>
- [86] S. S. Tannu and M. K. Qureshi, “Not all qubits are created equal: a case for variability-aware policies for nisq-era quantum computers,” in *Proceedings of the Twenty-Fourth International Conference on Architectural Support for Programming Languages and Operating Systems*, 2019, pp. 987–999.
- [87] Y. Ueno, M. Kondo, M. Tanaka, Y. Suzuki, and Y. Tabuchi, “Qulatis: A quantum error correction methodology toward lattice surgery,” in *2022 IEEE International Symposium on High-Performance Computer Architecture (HPCA)*. IEEE, 2022, pp. 274–287.
- [88] R. Versluis, S. Poletto, N. Khammassi, B. Tarasinski, N. Haider, D. J. Michalak, A. Bruno, K. Bertels, and L. DiCarlo, “Scalable quantum circuit and control for a superconducting surface code,” *Physical Review Applied*, vol. 8, no. 3, p. 034021, 2017.
- [89] L. Viola, E. Knill, and S. Lloyd, “Dynamical decoupling of open quantum systems,” *Physical Review Letters*, vol. 82, no. 12, p. 2417, 1999.
- [90] J. J. Wallman and J. Emerson, “Noise tailoring for scalable quantum computation via randomized compiling,” *Physical Review A*, vol. 94, no. 5, p. 052325, 2016.
- [91] H. Wang, Y. Ding, J. Gu, Y. Lin, D. Z. Pan, F. T. Chong, and S. Han, “Quantumnas: Noise-adaptive search for robust quantum circuits,” in *2022 IEEE International Symposium on High-Performance Computer Architecture (HPCA)*. IEEE, 2022, pp. 692–708.
- [92] H. Wang, J. Gu, Y. Ding, Z. Li, F. T. Chong, D. Z. Pan, and S. Han, “Quantumnat: Quantum noise-aware training with noise injection, quantization and normalization,” *arXiv preprint arXiv:2110.11331*, 2021.
- [97] H. Wang, B. Tan, P. Liu, Y. Liu, J. Gu, D. Z. Pan, J. Cong, and S. Han, “Q-Pilot: Field Programmable Quantum Array Compilation with Flying Ancillas,” in *arXiv preprint*, 2023.
- [93] H. Wang, Z. Li, J. Gu, Y. Ding, D. Z. Pan, and S. Han, “Qoc: quantum on-chip training with parameter shift and gradient pruning,” in *Proceedings of the 59th ACM/IEEE Design Automation Conference*, 2022, pp. 655–660.
- [94] H. Wang, P. Liu, J. Cheng, Z. Liang, J. Gu, Z. Li, Y. Ding, W. Jiang, Y. Shi, X. Qian *et al.*, “Quest: Graph transformer for quantum circuit reliability estimation,” in *IEEE/ACM International Conference on Computer-Aided Design (ICCAD)*, 2022.
- [95] H. Wang, P. Liu, Y. Liu, J. Gu, J. Baker, F. T. Chong, and S. Han, “DGR: Tackling Drifted and Correlated Noise in Quantum Error Correction via Decoding Graph Re-weighting,” in *arXiv preprint*, 2023.
- [96] H. Wang, P. Liu, K. Shao, D. Li, J. Gu, D. Z. Pan, Y. Ding, and S. Han, “Transformerqec: Transferable transformer for quantum error correction code decoding,” in *IEEE/ACM International Conference on Computer-Aided Design (ICCAD), FastML for Science Workshop*, 2023.
- [98] W. K. Wootters and W. H. Zurek, “A single quantum cannot be cloned,” *Nature*, vol. 299, no. 5886, pp. 802–803, 1982.
- [99] L. G. Wright, T. Onodera, M. M. Stein, T. Wang, D. T. Schachter, Z. Hu, and P. L. McMahon, “Deep physical neural networks trained with backpropagation,” *Nature*, vol. 601, no. 7894, pp. 549–555, 2022.
- [100] A. Wu, G. Li, H. Zhang, G. G. Guerreschi, Y. Ding, and Y. Xie, “A synthesis framework for stitching surface code with superconducting quantum devices,” in *Proceedings of the 49th Annual International Symposium on Computer Architecture*, ser. ISCA ’22. New York, NY, USA: Association for Computing Machinery, 2022, p. 337–350. [Online]. Available: <https://doi.org/10.1145/3470496.3527381>
- [101] X.-C. Wu, D. M. Debroy, Y. Ding, J. M. Baker, Y. Alexeev, K. R. Brown, and F. T. Chong, “Tilt: Achieving higher fidelity on a trapped-ion linear-tape quantum computing architecture,” *arXiv preprint arXiv:2010.15876*, 2020.
- [102] L. Xie, J. Zhai, Z. Zhang, J. Allcock, S. Zhang, and Y.-C. Zheng, “Suppressing zz crosstalk of quantum computers through pulse and scheduling co-optimization,” in *Proceedings of the 27th ACM International Conference on Architectural Support for Programming Languages and Operating Systems*, 2022, pp. 499–513.
- [103] M. Xu, Z. Li, O. Padon, S. Lin, J. Pointing, A. Hirth, H. Ma, J. Palsberg, A. Aiken, U. A. Acar, and Z. Jia, “Quartz: superoptimization of quantum circuits,” in *Proceedings of the 43rd ACM SIGPLAN International Conference on Programming Language Design and Implementation*, 2022, pp. 625–640.
- [104] B. Zhang, S. Majumder, P. H. Leung, S. Crain, Y. Wang, C. Fang, D. M. Debroy, J. Kim, and K. R. Brown, “Hidden inverses: Coherent error cancellation at the circuit level,” *arXiv preprint arXiv:2104.01119*, 2021.
- [105] C. Zhang, A. B. Hayes, L. Qiu, Y. Jin, Y. Chen, and E. Z. Zhang, “Time-optimal qubit mapping,” in *Proceedings of the 26th ACM International Conference on Architectural Support for Programming Languages and Operating Systems*, 2021, pp. 360–374.
- [106] X.-M. Zhang, T. Li, and X. Yuan, “Quantum state preparation with optimal circuit depth: Implementations and applications,” 2022. [Online]. Available: <https://arxiv.org/abs/2201.11495>
- [107] H. Zheng, G. S. Ravi, H. Wang, K. Setia, F. T. Chong, and J. Liu, “Sncqa: A hardware-efficient equivariant quantum convolutional circuit architecture,” in *2023 IEEE International Conference on Quantum Computing and Engineering (QCE)*, 2023.